

A Kinetic Study of the Mechanism of the Solid-State Reaction between Pyromellitic Dianhydride (PMDA) and Oxydianiline (ODA)

Christos D. Dimitrakopoulos* and Eugene S. Machlin

Henry Krumb School of Mines, Department of Chemical Engineering, Materials Science and Mining Engineering, Columbia University, New York, New York 10027

Steven P. Kowalczyk

IBM Research Division, T. J. Watson Research Center, P.O. Box 218, Yorktown Heights, New York 10598

Received November 21, 1995; Revised Manuscript Received May 31, 1996[®]

ABSTRACT: A kinetic study of the solid-state reaction between the polyimide precursor monomers PMDA and ODA has been carried out in the temperature range between -50 and $+23$ °C, using molecular beam deposition (MBD) for film growth and transmittance infrared spectroscopy (FTIR) for reaction monitoring. The product of this reaction consists mainly of dimers. Only 50% of the anhydride groups (two per PMDA molecule), contained in the film resulting from the stoichiometric codeposition of the monomers PMDA and ODA, form amide links by the end of the low-temperature reaction. The very low mobility of the reaction products below room temperature results in cessation of the solid-state reaction, when all PMDA monomers have reacted with only one of their anhydride rings. Formation of amine carboxylate complexes proceeds in parallel with amic acid formation. The measured values for the activation energy of the solid-state reaction between PMDA and ODA lie between 48 and 53 kJ/mol, which indicates that diffusion of monomers through the bulk of the film is the rate limiting step of this reaction.

I. Introduction

Aromatic polyimides (PI) are important dielectric materials for microelectronic applications.^{1,2} Low dielectric constant and high thermal stability are among their attractive properties.^{3a,c} The most widely used polyimide is poly(4,4'-oxydiphenylenepyrromellitimide), which results from the reaction of the monomers 1,2,4,5-benzenetetracarboxylic anhydride or pyromellitic dianhydride (PMDA) and bis(4-aminophenyl) ether or oxydianiline (ODA), and subsequent heat treatment of the product (Figure 1). The standard method for preparing thin films of polyimide in microelectronic applications is that of spin-coating a polyimide precursor, such as poly(amic acid) (PAA), from solution onto appropriate substrates, subsequently followed by thermal annealing to induce imidization.⁴ This is a simple process, but it utilizes solvents, that conceivably might be disadvantageous for some applications, particularly those requiring pinhole free ultrathin films with high thickness uniformity.

Vapor codeposition of the monomers in vacuum is an alternative method for producing PI films. A vapor deposition technique for PI film growth was first studied by Salem et al.⁵ and Iijima et al.^{6,7} Shortly after, this technique was further developed for production of ultrathin films in ultrahigh vacuum (UHV), for in situ interfacial chemistry studies^{8–13} and studies on the role of solvents in interfacial reactions.¹⁴ A study of the key growth parameters for the preparation of uniform, high-quality, relatively thick PI films by vapor deposition was presented later.^{15,16}

From the very first applications of the vapor deposition method for production of PMDA–ODA polyimide films, it was observed using FTIR spectroscopy that the as-deposited film was a mixture of reacted and unre-

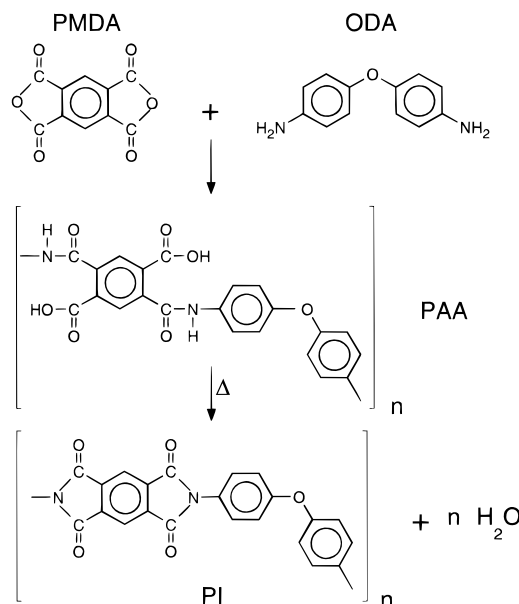


Figure 1. Scheme of the reaction in solution between PMDA and ODA to produce poly(amic acid) (PAA) and after annealing polyimide (PI).

acted species, when the substrate was kept at room temperature during deposition.^{5,7} Hahn et al.,¹⁷ using in situ IR reflectance spectroscopy, have studied the chemistry of the reaction of the two monomers in the solid state, in the temperature range from -53 to $+242$ °C. The main idea included in their proposed scheme was the formation of an amine carboxylate salt. This was actually proposed earlier by the same group on the basis of XPS results.¹⁸ According to this model, in order to form a carboxylate salt two amine moieties from different ODA molecules are consumed to react with an anhydride ring.

To the best of the authors' knowledge no study of the kinetics of the solid-state reaction between PMDA and

* Present address: IBM Research Division, T. J. Watson Research Center, P.O. Box 218, Yorktown Heights, NY 10598.

[®] Abstract published in *Advance ACS Abstracts*, August 1, 1996.

ODA or similar monomers has been published. In this work we study the kinetics of the solid-state reaction in the temperature range from $-50\text{ }^{\circ}\text{C}$ (where, practically, reaction products start forming) to room temperature, in order to provide data that may help bring about an understanding of the mechanism of this reaction.

II. Experimental Section

A. Molecular Beam Deposition. The deposition system has been described previously.^{15,16,19} The deposition controllers connected to programmable power supplies ensure that the desired deposition rates can be controlled accurately for both monomers and remain constant despite changes in the total surface area of the monomer crystals in the sources during deposition (both monomers sublimate).

During a typical deposition run the base pressure of the chamber was below 2×10^{-7} Torr. A base pressure of 1×10^{-8} Torr could be achieved after a short bake-out of the chamber. Before initiation of growth, the molecular fluxes from each of the monomer sources were stabilized to their calibrated stoichiometric ratio, with the substrate shuttered. Pressure during deposition was 8×10^{-7} to 6×10^{-6} Torr. Deposition rates were in the range from 0.1 to 0.5 nm/s, although higher rates were easily achievable. The films used in the kinetics experiments had a thickness of 270 nm.

B. Kinetics Experiment. A large amount of reaction product is already formed at the end of monomer codeposition at room temperature, or after deposition on a cooled substrate which is then allowed to reach room temperature. In order to study the solid-state polymerization reaction kinetics, the films had to be deposited at substrate temperatures below $-100\text{ }^{\circ}\text{C}$, where reaction does not occur. In this way, the initial stages of the reaction after completion of the deposition could be monitored. A specially designed substrate holder enabled accurate control of the sample temperature from $-170\text{ }^{\circ}\text{C}$ to room temperature.¹⁶ Fast response times for temperature changes were achieved and temperature could be set within $\pm 0.1\text{ }^{\circ}\text{C}$.

Transmittance FTIR spectroscopy was used to monitor changes in the concentrations of appropriate moieties in the film. It allowed for fast, repetitive measurements with small time intervals. It is vacuum compatible, nondestructive and, unlike techniques using X-rays,¹² does not interfere with the reaction process.

A special detachable chamber containing the sample holder was employed to allow for the placement of the sample in the IR-beam path, while it remained in high vacuum.¹⁶ During transfer to the spectrometer and during characterization the sample should not be exposed to ambient atmosphere. Humidity in air hydrolyzes the unreacted portion of PMDA (see Figures 3 and 4 in next section) and already formed amic acid.⁴

CaF_2 windows, which transmit IR radiation above 1000 cm^{-1} frequency with high efficiency, were used for the detachable chamber. An IBM IR-98 FTIR spectrometer with a vacuum bench and a liquid nitrogen cooled MCT detector for the mid-IR frequency range was used. The substrates were 1 in. undoped silicon wafers with a 1° wedge shape and double-polished surfaces. They were purchased from Harrick Scientific.

For FTIR characterization other than the kinetics experiments a Nicolet 740 FTIR spectrometer with a nitrogen-purged bench and a liquid N_2 cooled MCT detector was used.

III. Results and Discussion

A. FTIR Spectra. Assignment of the peaks of the IR spectrum of PI has been reported earlier.²⁰ In Figure 2 the FTIR spectrum of a PMDA-ODA film deposited at $-100\text{ }^{\circ}\text{C}$ and then annealed at $-28\text{ }^{\circ}\text{C}$ for a few hours is shown. The assignment of the numbered IR peaks appearing in Figure 2 is given in Table 1 and was made

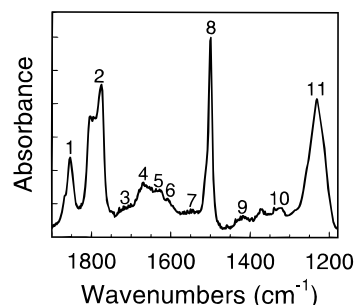


Figure 2. IR spectrum of a 270 nm thick PMDA-ODA film deposited at $-100\text{ }^{\circ}\text{C}$ and then left at $-28\text{ }^{\circ}\text{C}$ for a few hours.

Table 1. Assignment of the Peaks Appearing in the FTIR Spectrum of an As-Deposited PMDA-ODA Film, at or below Room Temperature

no.	frequency (cm^{-1})	vibrational mode
1	1850	anhydride ring symmetric carbonyl stretching
2	1790	anhydride ring asymmetric carbonyl stretching
3	1710	amic acid carbonyl stretching
4	1670	amide carbonyl stretching
5	1627	ODA aromatic ring mode
6	1607	asymmetric stretch of the carboxylate ion (COO^-)
7	1545	amide N-H bending mode
8	1500	ODA aromatic ring mode (ν_{13})
9	1410	symmetric stretch of the carboxylate ion (COO^-)
10	1325	amide C-N stretching mode
11	1240	ether C-O-C and anhydride C-O-C stretching

according to refs 17 and 18. Features attributed to the reaction products and the reactants are clearly apparent.

The major complication in characterizing the as-deposited PMDA-ODA films using FTIR is that there is no clear indication for the concentration of the unreacted ODA present in the film, as opposed to the case of PMDA, which presents intense and well-separated peaks of the anhydride carbonyl stretching modes. The prominent peaks due to ODA are mainly attributed to the phenyl ring vibrational modes and thus are not affected by any reaction of the amine end groups. When ODA and PMDA are codeposited on a substrate, the region between 3300 and 3500 cm^{-1} , where the primary amine stretching modes normally appear, exhibits two very broad bands,^{17,16} which are not useful for quantitative measurements. These bands are broadened and lose intensity as compared to the pure ODA films, due to the perturbation of the ODA molecules when codeposited with PMDA,¹⁷ mainly due to the various kinds of neighboring moieties to the amine groups.

In order to ensure that the existence of unreacted anhydride moieties in the film was not due to a deviation from stoichiometry but had remained unreacted despite the simultaneous presence of unreacted amine moieties in the film, films with a large excess of ODA were deposited and characterized with FTIR spectroscopy. Even at high ODA contents (70 mol %) unreacted anhydride was observed in the as-deposited state.

MBD PMDA films can be hydrolyzed by humidity in the air. This was exhibited by depositing PMDA on an undoped Si wafer and recording its transmittance IR spectra immediately after deposition and after exposure to air for 44 h (Figure 3). A new peak appears between 1700 and 1730 cm^{-1} in the latter spectrum (marked with an arrow in Figure 3) and is assigned to the carbonyl stretch of pyromellitic acid. The amic acid carbonyl

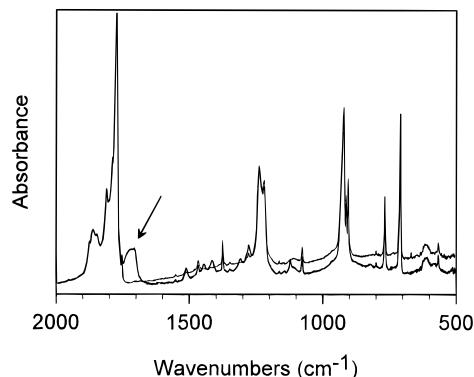


Figure 3. IR spectra of an 800 nm thick PMDA film on an undoped Si wafer, taken immediately after deposition and after exposure to air for 44 h.

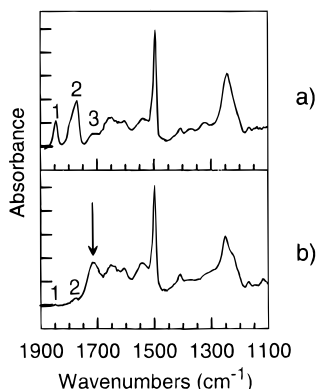


Figure 4. IR spectra from two pieces of the same MBD PMDA-ODA film (a) after 22 days in N_2 atmosphere and (b) after 22 days in air.

stretch peak appears also in the same frequency range in the case of codeposited PMDA-ODA. An as-deposited PMDA-ODA film left in nitrogen for 22 days (Figure 4a) showed intense anhydride peaks, while a piece of the same sample left in air for the same period of time showed minuscule anhydride peaks and a large peak at the area where the pyromellitic acid carbonyl peak appears (Figure 4b). The numbers appearing on the peaks in Figure 4a,b correspond to the vibrational modes listed in Table 1. The arrow in Figure 4b shows the position of the pyromellitic and amic acid carbonyl peaks. This proves that the increase of the intensity of the acid carbonyl peak in the film that was stored in air is not due to progress of the reaction between PMDA and ODA but due to hydrolysis of unreacted anhydride moieties by ambient humidity. This is also supported by the practically equal intensity of the amide carbonyl peak of the two samples at around 1670 cm^{-1} . These results show the importance of keeping the sample in a humidity-free environment before or during the kinetics experiment.

Because some of the peaks of interest in the FTIR spectra were overlapping with neighboring peaks, peak analysis was performed.²¹ In this way, the intensity of the amide carbonyl stretching peak at 1670 cm^{-1} , which overlaps with two other peaks, could be monitored. The integrated intensity of this peak, I_{AM} , is proportional to the concentration of amide links in the film, which in turn is a clear indication of PMDA and ODA monomer amidization reaction. For monitoring the anhydride concentration throughout the reaction the asymmetric and symmetric anhydride carbonyl stretching peaks were used. They appear at 1790 and 1850 cm^{-1} , respectively. These are high-intensity peaks; thus the

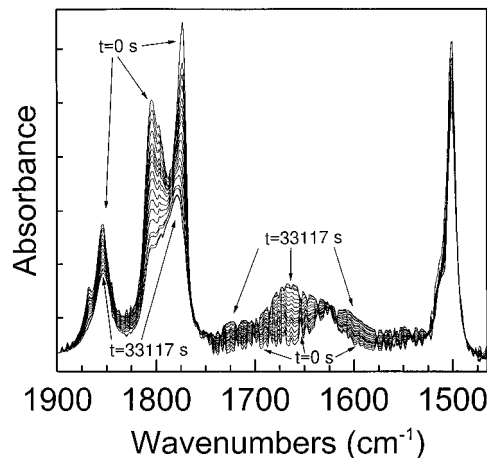


Figure 5. Sequence of IR spectra taken at different times during an isothermal experiment at $T_2 = -28\text{ }^\circ\text{C}$, which lasted 33 117 s.

effect of noise is negligible. They do not overlap with any other peaks but themselves. In order to monitor changes in anhydride concentration with time, one can either plot the intensity of each peak separately vs time, which requires peak analysis to separate their overlapping tails, or plot the cumulative intensity of both peaks vs time. As shown in Figure 7 the results are equivalent. The sum of the integrated intensities of the two anhydride peaks is denoted by I_{AN} . A small systematic error occurs in the measurement of the intensity of each anhydride peak separately, due to the peak analysis process, which always leaves a small part of the area around 1834 cm^{-1} unaccounted for. This is the region where the tails of the two peaks overlap (Figure 6). This error is eliminated when the sum of the intensities of both peaks is used. For this reason I_{AN} is considered the most reliable monitor of the reaction rate.

The amide C-N stretch peak that appears at around 1325 cm^{-1} is also a clear indication of amide formation but is too small to be good for reliable quantitative measurements. Besides, there is an overlap with another small peak whose intensity changes during the reaction.

The sum of the integrated intensities of the anhydride carbonyl stretching peaks at $-100\text{ }^\circ\text{C}$, I_{AN}^0 , provides the starting concentration of anhydride rings on PMDA molecules in the as-deposited films, in arbitrary units. At this temperature no reaction has taken place after the end of deposition, and thus the integrated intensity of the amide carbonyl stretching peak, I_{AM}^0 , is zero. I_{AN} should go to zero upon completion of the polymerization reaction and the ratio of I_{AN} to I_{AN}^0 at any time t measures the portion of anhydride rings that remains unreacted.

Instead of plotting integrated intensity versus time, the measured values can be normalized with respect to I_{AN}^0 and plots of conversion factor or fractional conversion vs time can be used. In this way, all plots are normalized to an ordinate range from 0 to 1. The fractional conversion of a reactant (or conversion factor) is given by²²

$$X_{AN} = \frac{I_{AN}^0 - I_{AN}}{I_{AN}^0} \quad (1)$$

In the case of the product phase, the fractional conversion can be calculated if the integrated intensity of the amide carbonyl peak after all reactants have reacted,

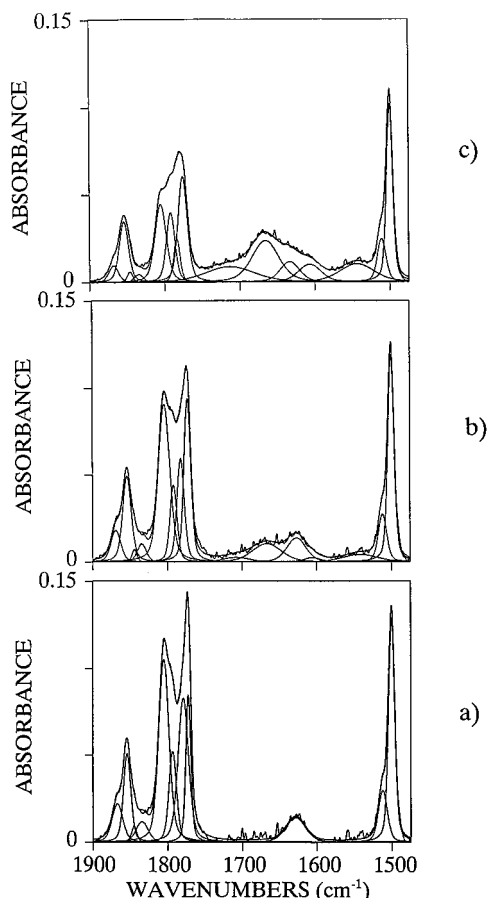


Figure 6. Illustration of the peak analysis process: (a) the IR spectrum of a totally unreacted, as-deposited PMDA-ODA film taken at $-100\text{ }^{\circ}\text{C}$ which is used as the zero fractional conversion point; (b) spectrum taken during the intermediate stage of the isothermal reaction at $-8\text{ }^{\circ}\text{C}$; and (c) spectrum from the same isothermal experiment taken when the reaction rate has been practically reduced to zero. Each figure shows the original spectrum (noisy line), the calculated best fit (smooth line superimposed on the real spectrum), and the individual peaks whose summation produces the best fit.

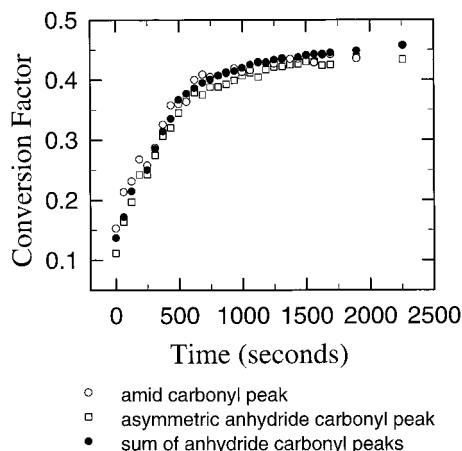


Figure 7. Plots of the conversion factor as calculated by three different measurements, namely I_{AM} , I_{AN} , and asymmetric carbonyl peak integrated intensity vs time for the $T_1 = -8\text{ }^{\circ}\text{C}$ isothermal.

$I_{AM}^{100\%}$, is known. The conversion factor for the product is defined according to the formula

$$X_{AM} = \frac{I_{AM}}{I_{AM}^{100\%}} \quad (2)$$

In these experiments, the end concentration of the

product was not known, because the reaction was not completed under the conditions used. Instead, the fractional conversion measured from the anhydride concentration after the reaction rate had become practically zero was assumed to be also the fractional conversion into product. This is a reasonable assumption, considering that the only way that the anhydride concentration can be reduced in the absence of water is through amidization.

With long time annealing at a constant temperature, T , between $-40\text{ }^{\circ}\text{C}$ and room temperature it has been found that the integrated intensities I_{AN} and I_{AM} approach a plateau value which is denoted by $I_y^{\infty}(T)$, where y stands for either AN or AM.

B. Results of Isothermal Measurements. A sequence of spectra taken at different times during the isothermal measurement at $T_2 = -28\text{ }^{\circ}\text{C}$ is shown in Figure 5. The gradual reduction of the symmetric and asymmetric anhydride carbonyl stretching peak intensities around 1850 and 1790 cm^{-1} and the gradual increase of the amide carbonyl stretching peak intensity around 1670 cm^{-1} and the amide N-H bending peak intensity at 1540 cm^{-1} , can be clearly seen. The intensity of the peak centered at 1606 cm^{-1} , which is due to the asymmetric stretching mode of COO^- , increases simultaneously with the intensity of the amic acid carbonyl stretching peak at 1710 cm^{-1} . This means that amine carboxylate salt formation and amic acid formation proceed simultaneously.

Figure 6 shows an example of the peak analysis process performed on each of the spectra taken during the kinetics experiment. Figure 6a shows the spectrum of a totally unreacted, as-deposited film taken at $-100\text{ }^{\circ}\text{C}$. There is no amide carbonyl stretching peak at 1670 cm^{-1} that would indicate any reaction between the monomers. This film was used for the isothermal run at $T_1 = -8\text{ }^{\circ}\text{C}$, and the results from the spectrum in Figure 6a were used as the zero fractional conversion point for this isothermal. In Figure 6b an intermediate stage of the isothermal reaction at $-8\text{ }^{\circ}\text{C}$ is shown, while Figure 6c corresponds to the final stage of the same isothermal, where the reaction rate had been practically reduced to zero. The anhydride carbonyl stretching peaks were best fitted by four peaks each, because both peaks have asymmetries and shoulders. All peaks are analyzed simultaneously at one run, because of overlaps between different peaks. Each point on a fractional conversion versus time curve (e.g. Figures 7, 8, 10, and 11.) corresponds to one spectrum.

Plots of consecutive spectra taken during the $T_1 = -8\text{ }^{\circ}\text{C}$ and $T_3 = -38\text{ }^{\circ}\text{C}$ isothermal runs exhibit similar behavior.

In Figure 7 we see plots of the conversion factor as calculated by three different measurements, namely I_{AM} , I_{AN} , and asymmetric carbonyl peak integrated intensity vs time for $T_1 = -8\text{ }^{\circ}\text{C}$. Good agreement was observed for all three.

Figure 8 shows the conversion factor, X_{AN} , vs time, t , plots for three isothermal runs at temperatures $T_3 = -38\text{ }^{\circ}\text{C}$, $T_2 = -28\text{ }^{\circ}\text{C}$, and $T_1 = -8\text{ }^{\circ}\text{C}$. The extent of the reaction at the beginning of each isothermal was different. This was due to the progress of the reaction during heating from $-100\text{ }^{\circ}\text{C}$ to T_z ($z = 1-3$). In the case of the lowest temperature isothermal, T_3 , no product was observed at the beginning of the isothermal. This was due to the short temperature ramp time and because T_3 is close to the temperature where reaction starts.

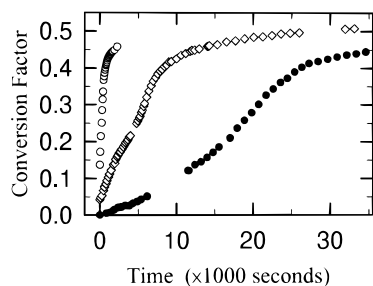


Figure 8. Plots of conversion factor vs time, for three isothermal runs at temperatures (●) $T_3 = -38$ °C, (◇) $T_2 = -28$ °C, and (○) $T_1 = -8$ °C.

It is apparent from the previous plot that the value of the conversion factor at the end of the reaction, when the reaction rate approaches zero, is about 0.5. Interestingly enough, this value did not change significantly when the temperature was raised to room temperature at the end of each isothermal run.

Here, it should be stressed that what is really measured by monitoring the anhydride carbonyl peaks with FTIR, is the concentration of the anhydride functional groups (two per PMDA molecule). Thus, even if every PMDA molecule reacts with one ODA molecule to form dimers, the FTIR peak analysis would reveal the 50% of the anhydride groups that remain as unreacted end groups of the dimers. The only way that an anhydride ring can be consumed in a water-free environment, is by reacting with an amine group to form an amide link. The amine group can belong to either an ODA molecule that has reacted at one side only or an unreacted ODA. Hence, the number of amide links formed is equal to the number of anhydride rings consumed.

This is not the case for the amine functional groups of ODA (two per ODA molecule). Some of the reacted anhydride groups form an amine carboxylate salt besides forming an amide linkage (Figure 9, structure I).^{17,18} Hence, two amine groups belonging to two different ODA molecules are consumed by each of these anhydride groups. Eventually, a deficiency of amine groups is created relative to anhydride. Thus, there will be some PMDA monomers that will not be able to find an ODA monomer to react with and form a dimer. Each of these excess PMDA monomers might react with the amine end group of a PMDA-ODA dimer to form a PMDA/ODA/PMDA trimer or with the amine end group of an ODA monomer that has already formed an amine carboxylate complex. Structure II in Figure 9 illustrates a combination of both of these reaction products. If this was not the case, a concentration of unreacted PMDA larger than 50% would be measured (or the conversion factor would be below 0.5). The difference from the 50% concentration would be proportional to the concentration of amine carboxylate complexes.

At this stage, where each PMDA molecule reacts through only one of its anhydride groups, there are still unreacted anhydride carbonyl groups and unreacted amine groups that upon reaction would form higher n -mers ($n \geq 3$). Such reactions would obviously increase the conversion factor of anhydride carbonyl groups above 0.5. Since this result has never been observed for films heated to room temperature, it may be concluded that no higher n -mers than trimers are formed in the reactions between PMDA and ODA at this temperature range.

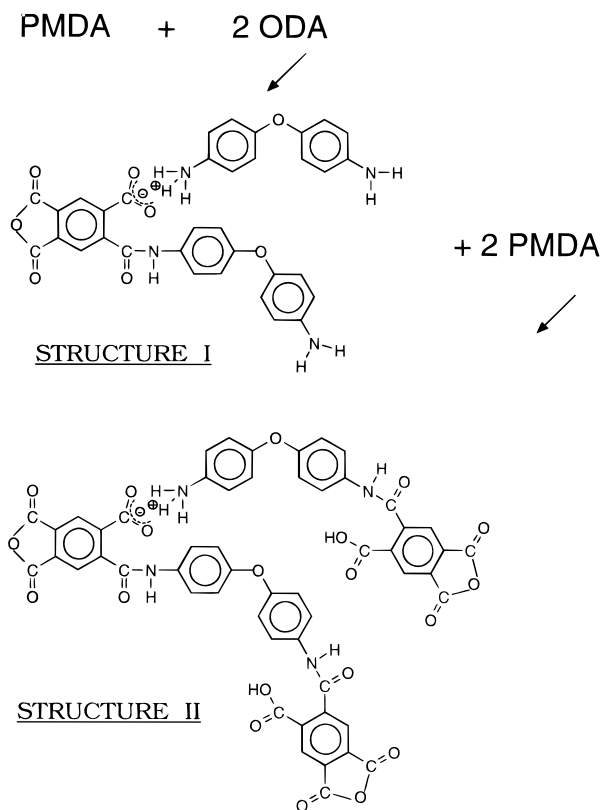


Figure 9. Formation of an amine carboxylate salt complex (structure I), and further reaction with PMDA monomers to form a larger oligomer (structure II).

Another set of products, which would produce the observed conversion factor of 0.5 at the plateau stage of the reaction for temperatures below 25 °C, is a mixture of poly(amic acid) (PAA) macromolecules and unreacted ODA and PMDA monomers; 50% of the PMDA monomers and 50% of the ODA monomers minus the ODA molecules that have formed amine carboxylate complexes would be unreacted. Contributions to these concentrations from the end groups of the polymer chains are too small due to the assumed large length of the polymer chains (relatively small number of very long chains) and can be ignored. However, the possibility that those are the products of the reaction can be ruled out. The monomers that remain unreacted should readily react with available counterpart monomers or end groups of longer molecules. Thus, the reaction would not stop at this stage and an anhydride concentration much smaller than 50% would be measured at the plateau stage. Coexistence of both monomers at the plateau stage would be feasible only if phase separation of PMDA or ODA occurred. If ODA were phase separated, four sharp peaks due to the two N-H stretching modes of ODA around 3350 and 3450 cm^{-1} should be observed at room temperature. These should be split due to the intermolecular interactions in well-ordered ODA phases.^{16,17} Although MBD ODA films tend to become highly ordered at and below room temperature,^{16,17} the above-mentioned peaks were not observed in the spectra of codeposited PMDA-ODA films. The existence up to 142 °C of large concentrations of anhydride groups in MBD films of PMDA-ODA and the detection of some anhydride groups even at 182 °C¹⁷ indicate that PMDA phase separation does not occur. These films were annealed in vacuum and thus any unreacted PMDA molecules would have sublimed at

around 37 °C. This is the desorption temperature for PMDA monomer.^{16,17} This clearly suggests that the measured IR intensity due to anhydride functional groups should be attributed to end groups of monoaminated PMDA, not unreacted PMDA monomers. Larger molecules desorb at higher temperature than the monomers, and they probably react further to produce polymer chains before they reach their sublimation temperature.

The reaction between an anhydride group and an amine group is reversible.^{3d} In this reaction, the condensation byproduct, the carboxyl group is chemically attached to the product; hence it cannot be physically removed in order to drive the reaction to completion.^{3d} However, when the reaction takes place in a polar aprotic solvent, which forms strong hydrogen bond complexes with the hydroxyl groups of the carboxyl groups, the reverse reaction is hindered, and high molecular weight poly(amic acid)s can be formed even when relatively low-basicity diamines or low-electrophilicity dianhydrides are used.^{3d} When ether or hydrocarbon solvents are used, the equilibrium constant is strongly dependent on the above-mentioned properties of the monomers.^{3d} Obviously, in the absence of solvent, as is the case in the solid-state reaction of PMDA and ODA, the equilibrium constant, and hence the molecular weight of the product, should be much lower than in the case of the same reaction in a polar aprotic solvent solution. In the latter case, the equilibrium constant is so high that the reaction has often been considered irreversible in the past.

Even small deviations from reactant stoichiometry can reduce dramatically the molecular weight of the product of the reaction. The consumption of two amine groups by one anhydride group when an amine carboxylate salt complex is formed results in a deviation from the stoichiometric ratio of the functional groups. This could be—at least partially—responsible for the low molecular weight of the solid-state reaction product.

Another potential explanation for the termination of the acylation reaction once all anhydride monomers have reacted with one side could be that the reactivity of the second anhydride group has been dramatically reduced to a point that no further reaction can take place at or below room temperature. The electron affinity, which is the experimentally determined quantitative measure of anhydride reactivity,^{3b} is reduced by 20% when PMDA monomer and monoaminated PMDA are compared.^{3b} According to ref 3b this is a small difference and thus the difference in acylation rates of the monomer and its monoaminated derivative should also be small. Indeed, the rate constants for acylation of PMDA with ODA in solution before and after 50% conversion of functional groups were 9 and 6 L mol⁻¹ s⁻¹, respectively, and high molecular weight polymer is produced at room temperature.^{3b} After consideration of kinetic data it was concluded that in solution “the reactivity of terminal functional groups is practically equivalent to that of the reactive sites of the monomers in the formation of the majority of polyamic acids” including PMDA–ODA.^{3b} These results indicate that differences in the reactivity of the end groups of the monomers and the dimers or structure II molecules are not responsible for the cessation of the reaction at 50% conversion.

The reactant molecules are in a film that is more than one monolayer thick. Thus, they must diffuse in the bulk of this film for reaction to occur. The increased

size of the reaction products will reduce their mobility relative to the monomers. It has been reported previously that the diffusion coefficient is dependent on the molecular structure of the diffusing molecule (small organic molecules in rubbers).²³ This dependence is best represented by an effective molecular diameter, which is the weighted average of the three major molecular dimensions, with the importance of each dimension of the diffusing molecule being inversely proportional to its length.²² The natural logarithm of the diffusion coefficients of six different organic solvents in natural rubber was shown to be linearly dependent on the volume of a sphere with the above mentioned diameter (effective volume).²² By making Arrhenius plots of the temperature dependence of these diffusion coefficients (reported in Table 1 of ref 22) we could see that the activation energy for diffusion ranges from 30 to 40 kJ/mol and also increases linearly with the effective volume.

The dimer, trimer, and structure II (Figure 9) molecules are longer and have substantially larger cross sections than the monomers. The reaction products should therefore have higher activation energies for diffusion than the monomers. This lack of mobility inhibits the favorable positioning of the reactive end groups of the two reaction products and prevents the reaction between the end groups of the reaction products; therefore no chain extension takes place in the solid state below room temperature. According to the above discussion, the maximum size structure for the reaction product would be structure II (Figure 9).

In polar solvents (e.g. *N*-methylpyrrolidone), the reaction between PMDA and ODA produces high molecular weight polymer.^{3d} The reactive end groups of the reaction products participate continuously in the acylation reaction. Their mobility in the liquid phase is much higher than in the solid state. In the solid state, the cessation in the reaction between anhydride and amine end groups of the reaction products, which occurs at conversion factor 0.5 at and below room temperature, could be attributed to the reduced mobility of the dimer, trimer, and structure II molecules as compared to that of the monomer molecules.

In the following section experimental measurements of the activation energy for the solid-state reaction between PMDA and ODA below room temperature are used to substantiate this argument.

C. Activation Energy for the Solid-State Reaction between PMDA and ODA at $T < 23$ °C. A knowledge of the value of the activation energy at different stages of the reaction can provide valuable information regarding the mechanism of the low-temperature acylation reaction. Activation energy measurements were obtained using the method of temperature jumps (T jumps), which relates the rate of change of reactant or product concentration (I_y , where y stands for either AN or AM) with time just before and just after a small increment or decrement of the temperature of the sample. This function, $(dI_y/dt)_T$, is continuous at a constant temperature $T = T_1$. After the system has attained equilibrium at the new temperature $T = T_2$, a new rate is measured. The method has been used extensively in the case of polymers for thermogravimetric studies of polymer decompositions.^{24,25} The activation energy (Q) of the process at the point of the jump can be calculated from the following equation:^{23,24}

$$Q = \frac{RT_1T_2}{T_2 - T_1} \ln \left[\frac{\left(\frac{dI_y}{dt}\right)_{T_2}}{\left(\frac{dI_y}{dt}\right)_{T_1}} \right]$$

The advantage of this method is that one does not have to compare results from different samples in order to determine the activation energy. This eliminates potential errors resulting from differences in the history of the samples. A difference in activation energy measured at different conversion factors would indicate changes occurring in the reaction process or the step controlling the kinetics of the reaction at different stages of the reaction. A single activation energy measured at different conversions would indicate that the same mechanism applies to the whole extent of the conversion factor range where Q was measured.

Figure 10 shows two T jumps which independently provide values of the activation energy close to the maximum reaction rate (just after it) and deep into the deceleratory stage of the reaction. The first jump occurred from -38 to -28 °C and the second from -28 to -38 °C.

In order to determine the rates of the reaction immediately before and after the T jump, a regression analysis of the last few points on each side of the jump was used. Then the slopes of the two regression lines were calculated at the point of the T jump. The points of the jumps are shown in the Figure 10 with arrows. The arrow on the left corresponds to the -38 to -28 °C T jump and the vertical arrow to the -28 to -38 °C T jump. The straight lines indicate the slope before and after each T jump. The time from the beginning of the T jump up to the stabilization of the new temperature was less than 5 min. This is an adequately short time—for the used temperature range—to ensure reliable results, since the conversion factor does not change significantly during the jump and until the system has stabilized at the new temperature.

The activation energy calculated from the first jump was 53 kJ/mol, and from the second jump 52 kJ/mol. They are very close indeed. There must be an error involved in these values, containing contributions from the not instant change in temperature and the standard error of the regression analysis, but this error appears to be small. The insensitivity of the activation energy value to the stage of the reaction indicates that there is a single mechanism that governs the kinetic behavior of the solid-state reaction at or below room temperature.

Figure 11 shows a T jump from -8 to $+9$ °C. The same method as before was used for the calculation of the activation energy and the resulting value was 48 kJ/mol, again very close to the Q values measured from Figure 10. The position of the T jump is indicated by an arrow, while the straight lines indicate the slope before and after the T jump.

The activation energy (Q) for reaction between PMDA and ODA in N,N -dimethylformamide (DMFA), is equal to 6.7 kJ/mol.²⁶ This value is more than 7 times smaller than the Q values we measure for the reaction of these monomers in the solid state. This difference can be attributed to the large difference in mobility of the reactive species in solution and in the solid state. Hence, the most possible rate limiting step for the low-temperature solid-state reaction between PMDA and ODA molecules is that of diffusion and alignment of

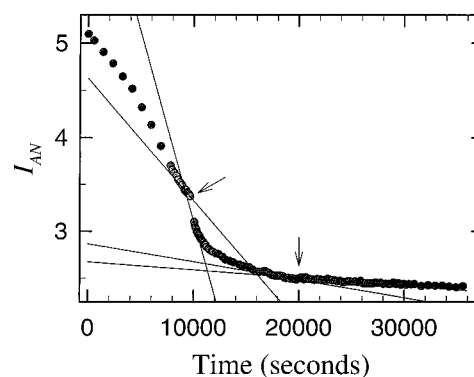


Figure 10. I_{AN} vs time plot from a temperature jump experiment.

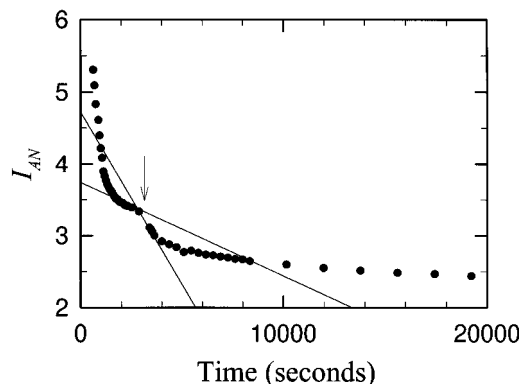


Figure 11. I_{AN} vs time plot from the -8 to $+9$ °C temperature jump experiment.

these reactants in the bulk of the MBD film, prior to the chemical attachment step.

In the course of bulk diffusion, the molecules are bound to each other only by van der Waals type forces; i.e. no covalent links need to be broken. In the literature there are numerous examples of solid-state diffusion of organic compounds in organic polymer matrices.^{27,28} The vast majority of reported values for activation energy for diffusion in such systems lie between 30 and 75 kJ/mol. The measured value for the activation energy of the solid-state reaction between PMDA and ODA lies at the center of this range. The major point in relating the solid-state diffusion of PMDA and ODA molecules in films of codeposited PMDA–ODA, to the diffusion of other organic molecules in polymers is that in all these systems the intermolecular forces involved are of the same type. Hence, one would expect that the activation energies for diffusion should be of the same order. The limited spread of these values should be attributed to the different shape and size of the molecules involved.

As mentioned in the previous section, the reaction products have lower mobilities than the monomers due to their increased size. As a result, at and below room temperature the reaction terminates when all monomers are consumed. From the fact that the measured activation for reaction in the solid state is comparable to the activation energy for diffusion of organic molecules in polymers, while at the same time it is 7 times higher than the activation energy for reaction between PMDA and ODA in solution, we must conclude that the rate limiting step in the reaction between PMDA and ODA monomers to form amide links in the solid state is more likely to be solid-state diffusion than it is to be the step of forming the link.

IV. Conclusions

The kinetics of the low-temperature solid-state reaction between PMDA and ODA have been studied for the first time. The product of this reaction up to room temperature consists mainly of dimers. The formation of amine carboxylate salts proceeds in parallel with amic acid formation. The measured activation energy value for solid-state reaction indicates that the rate limiting step of the reaction process is diffusion of the monomers through the bulk of the film that is formed during monomer codeposition at temperatures below -100°C .

Acknowledgment. We would like to thank Prof. D. Maroudas of U.C. Santa Barbara and Dr. G. Hougham of IBM Research for useful discussions, Dr. A. G. J. Staring of Philips Research for reviewing this document, and Mr. P. Lauro for helping in the design and construction of parts of the vacuum system. C.D.D. thanks IBM Research for the award of an IBM Manufacturing Research Fellowship.

References and Notes

- (1) Wilson, A. M. In *Polyimides: Synthesis, Characterization, and Applications*; Mittal, K. L., Ed.; Plenum Press: New York, 1984; Vol. 2, p 715.
- (2) (a) Jensen, R. J.; Cummings, J. P.; Vora, H. *IEEE Trans. Comp. Hybrids Manufact. Technol. CHMT* **1984**, *7*, 384. (b) Feger, C.; Feger, C. In *Multichip Module Technologies and Alternatives*; Doane, D. A., Franzon, P. D., Eds.; Van Nostrand Reinhold: New York, 1993.
- (3) (a) Bessonov, M. I.; Koton, M. M.; Kudryavtsev, V. V.; Laius, L. *Polyimides: Thermally Stable Polymers*; Consultants Bureau: New York, 1987. (b) *Ibid.*, pp 15, 23–26. (c) Wilson, D.; Stenzenberger, H. D.; Hergenrother, P. M. *Polyimides*; Chapman and Hall: New York, 1990. (d) Harris, F. W. In *Polyimides*; Wilson, D., Stenzenberger, H. D., Hergenrother, P. M., Eds.; Chapman and Hall: New York, 1990; pp 2–3. (e) *Ibid.*, p 5.
- (4) Sroog, C. E. *J. Polym. Sci., Macromol. Rev.* **1976**, *11*, 161.
- (5) Salem, J. R.; Sequeda, F. O.; Duran, J.; Lee, W. Y.; Yang, R. M. *J. Vac. Sci. Technol.* **1986**, *A4*, 369.
- (6) Iijima, M.; Takahashi, Y.; Inagawa, K.; Itoh, A. *J. Vac. Soc. Jpn.* **1985**, *28*, 437 (in Japanese).
- (7) Takahashi, Y.; Iijima, Y.; Inagawa, K.; Itoh, A. *J. Vac. Sci. Technol.* **1987**, *A5*, 2253.
- (8) Grunze, M.; Lamb, R. N. *J. Vac. Sci. Technol.* **1987**, *A5*, 1695.
- (9) Lamb, R. N.; Baxter, J.; Grunze, M.; Kong, C. W.; Unertl, W. N. *Langmuir* **1988**, *4*, 249.
- (10) Mack, R. G.; Grossman, E.; Unertl, W. N. *J. Vac. Sci. Technol.* **1990**, *A8*, 3827.
- (11) Kowalczyk, S. P.; Jordan-Sweet, J. L. *Chem. Mater.* **1989**, *1*, 592.
- (12) Kowalczyk, S. P. In *Metallization of Polymers*; Sacher, E., Pireaux, J.-J., Kowalczyk, S. P., Eds.; American Chemical Society: Washington, 1990; p 10.
- (13) Kowalczyk, S. P.; Stafstrom, S.; Bredas, J. L.; Salaneck, W. R.; Jordan-Sweet, J. L. *Phys. Rev. B* **1990**, *41*, 1645.
- (14) Kowalczyk, S. P.; Kim, Y.-H.; Walker, G. F.; Kim, J. *Appl. Phys. Lett.* **1988**, *52*, 375.
- (15) Kowalczyk, S. P.; Dimitrakopoulos, C. D.; Molis, S. *Mater. Res. Soc. Symp. Proc.* **1991**, *227*, 55.
- (16) Dimitrakopoulos, C. D. Ph.D. Thesis, Columbia University, 1993.
- (17) Hahn, C.; Strunskus, T.; Frankel, D.; Grunze, M. *J. Electron Spectrosc. Relat. Phenom.* **1990**, *54/55*, 1123.
- (18) Strunskus, T.; Grunze, M.; Gnanarajan, S. In *Metallization of Polymers*; Sacher, E., Pireaux, J.-J., Kowalczyk, S. P., Eds.; American Chemical Society: Washington, 1990; p 353.
- (19) Dimitrakopoulos, C. D.; Kowalczyk, S. P.; Lee, K.-W. *Polymer* **1995**, *36*, 4983.
- (20) Ishida, H.; Wellenhoff, S. T.; Baer, E.; Koenig, J. L. *Macromolecules* **1980**, *13*, 826.
- (21) The Spectra Calc software package was used (Galactic Industries Corp.).
- (22) Levenspiel, O. *Chemical Reaction Engineering*, 2nd ed.; John Wiley & Sons, Inc.: New York, 1972; p 46.
- (23) Guo, C. J.; De Kee, D.; Harrison, B. *Chem. Eng. Sci.* **1992**, *47*, 1525.
- (24) Flynn, J. H.; Dickens, B. *Thermochim. Acta* **1976**, *15*, 1.
- (25) Dickens, B. In *Degradation and Stabilization of Polymers*; Jellinek, H. H. G., Ed.; Elsevier: Amsterdam, 1983; p 554.
- (26) Moiseev, V. D.; Avetisyan, N. G.; Chernova, A. G.; Atrushkevich, A. A. *Plast. Massy* **1971**, No. 3, 12–13. Translated in *Sov. Plast. (Engl. Transl.)*.
- (27) Flynn, J. H. *Polymer* **1982**, *23*, 1325.
- (28) Doong, S. J.; Ho, W. S. W. *Ind. Eng. Chem. Res.* **1992**, *31*, 1050.

MA951728G